

# Characteristics of $\text{PbTiO}_3$ thin films on Pt/Ti/SiO<sub>2</sub>/Si by continuous cooling process

Y. S. YOON\*, J. H. KIM, W. K. CHOI

Division of Ceramics, Korea Institute of Science and Technology, P.O. Box 131 Cheongryang, Seoul, 130-650, South Korea

S. J. LEE

Department of Material Science and Engineering, University of Urbana-Champaign, Urbana, IL, 61801, USA

In order to introduce a new deposition process for ferroelectric thin film, the deposition temperature was continuously cooled down from 580 °C to 400 °C during the deposition which we call "continuous cooling process (CCP)". X-ray diffraction patterns showed that the  $\text{PbTiO}_3$  thin films deposited by the CCP and at 480 °C had polycrystallinity, but at substrate temperatures of 400 °C and 580 °C had poor crystallinity. Scanning electron microscopy of the CCP-deposited film surface showed larger granular-like micrograins than that of the film deposited at 480 °C and smaller than that of the film at 580 °C. While there was no other phase formation at the  $\text{PbTiO}_3$ -Pt interface in the CCP-deposited film, resulting in a sharp interface, there was severe interface reaction at the  $\text{PbTiO}_3$ -Pt and the Pt-Si in the film deposited at 580 °C, resulting in an abrupt interface. Atomic force microscopy under ambient conditions showed smoother surface of the film by the CCP than that of the films at 580 °C. Furthermore, the film by the CCP had higher packing density than that of the film at 480 °C. Besides enhancement of the structural properties, the CCP deposition appeared to have improved the electrical properties such as dielectric constant, dissipation factor, leak current density and polarization. In the case of the film by the CCP, polarization-electrical field measurement showed the saturation polarization of 27  $\mu\text{C cm}^{-2}$ , remanent of 14  $\mu\text{C cm}^{-2}$  and coercive of 150 kV. These results indicate that the CCP in metalorganic chemical vapour deposition has a possibility for fabrication of  $\text{PbTiO}_3$  ferroelectric thin films.

## 1. Introduction

Thin film growths of ferroelectric material on semiconducting wafers are particularly important for memory device applications, such as ferroelectric non-volatile random access memory (FRAM) and high density dynamic random access memory (DRAM) [1–5]. The ferroelectric thin films should meet some structural and electrical requirements such as defect free, low surface roughness, high dielectric constant, low dissipation factor, low leakage current and good polarization hysteresis behaviour. For example, large dielectric constant and/or large storage density are necessary for the DRAM devices. Particularly, a high value of remanent polarization ( $P_r$ ) is one of the most important electrical properties for FRAM devices. Recently, many research groups have reported on structural and electrical properties of  $\text{PbTiO}_3$  thin films in order to examine the possibility of memory device applications [6, 7]. It was suggested that film properties are strongly influenced by thin film deposition techniques and processes [8, 9]. For these reasons, growths of high quality ferroelectric thin film have

lead to investigation of many specific deposition methods and suitable deposition processes. Rapid advancements in the ferroelectric thin film deposition techniques, such as radio frequency (r.f.) sputtering [10] and metalorganic chemical vapour deposition (MOCVD) [11–17], have made it possible for ferroelectric thin films to be grown on semiconducting substrates. In order to grow the thin films with high quality, plasma enhancement or ion beam assistance were introduced in many vacuum deposition processes. However, such methods have disadvantages such as the high cost of the system. Furthermore, *in situ* deposition of high quality ferroelectric thin film on a metallic electrode coated-silicon substrate without deterioration of the base metallic electrode, at processing temperature of around 600 °C, has not been reported yet, to our best knowledge. Recently, many works on the process of ferroelectric thin film deposition have focused on selection of the base conducting electrode on Si wafer, such as Pt/Ti, Pt/Ta or RuO<sub>2</sub> [18, 19]. However, an optimal base conducting electrode material has not yet been reported. It was

\* Present address: Department of Electrical Engineering, Institute of Technology, University of Minnesota, 4-174 EE/CSci Building, 200 Union Street S.E., Minneapolis, MN55455.

suggested that the growth of ferroelectric thin films at low temperature is significantly important due to the interface reaction, such as non-conducting phase formation between the thin film and the base electrode or silicide formation, regardless of the base conducting electrode. Namely, the deposition of the ferroelectric thin film on the base conducting electrode coated-Si substrate suffer from the chemical reactions at relatively high temperature. Therefore, the growth of the ferroelectric thin films on a suitable base conducting electrode at relatively low substrate temperature is very important, particularly for the semiconducting process. It is, however, very hard to grow the high quality ferroelectric thin films on the base conducting electrode coated-Si substrate at low substrate temperatures compatible with the semiconducting process. In order to solve the above problems, we introduce a new deposition process.

In this study, we deposited the  $\text{PbTiO}_3$  thin films at various substrate temperatures. The deposition started at  $580^\circ\text{C}$  followed by a cooling to  $400^\circ\text{C}$  for 1 h. We termed this continuous cooling process (CCP) MOCVD. The concept of the CCP originated from the fact that the properties of the as-grown film are strongly influenced, not only by initial stage of film growth, but also by chemical reaction at the interface during the deposition. Structural and electrical properties of the  $\text{PbTiO}_3$  film by the CCP on Pt/Ti/SiO<sub>2</sub>/Si substrate were reported in order to examine the effects of the CCP on the film growth. From these results, we suggest that it may be possible to grow ferroelectric thin films by CCP for many applications.

## 2. Experimental procedure

Organometallic precursors were  $\beta$ -diketonate complex of  $\text{Pb}(\text{tmhd})_2$  (tmhd = 2,2,6,6-tetramethyl-3,5-heptanedione:  $\text{Pb}(\text{C}_{11}\text{H}_{19}\text{O}_2)_2$ ) and titanium tetraisopropoxide (TTIP:  $\text{Ti}(\text{OC}_3\text{H}_7)_4$ ). Fresh  $\text{Pb}(\text{tmhd})_2$  was used for every experimental run. Argon and pure oxygen gas was used as carrier and oxidizing gas, respectively. Table I shows the deposition conditions of MOCVD grown- $\text{PbTiO}_3$  thin films. The deposition was carried out for 60 min. In order to investigate continuous cooling effects on film formation, the deposition temperature was continuously cooled down from  $580^\circ\text{C}$  to  $400^\circ\text{C}$  during the deposition: we called this the continuous cooling process. After the deposition, the films were cooled down to room temperature

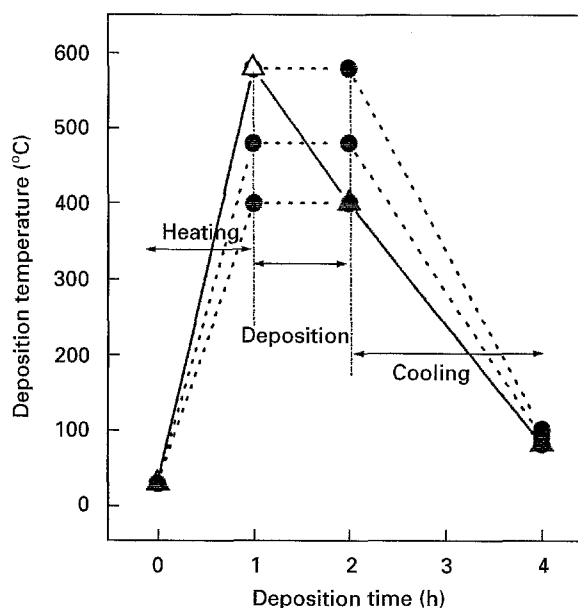


Figure 1 Schematic diagram of deposition processes for  $\text{PbTiO}_3$  films. (●) Common method; (Δ) CCP.

at a rate of  $150 \sim 200^\circ\text{C h}^{-1}$  under oxygen atmosphere. The deposition processes are shown in Fig. 1. Wavelength dispersive spectroscopy (WDS) with standard sample and Auger electron spectroscopy (AES) were employed to analyse the stoichiometry of the as-grown film. Characterization of crystallinity was identified by X-ray diffraction (XRD) and microstructures were examined by scanning electron microscopy (SEM). Root mean square (r.m.s.) roughness was calculated from two-dimensional atomic force microscopy (AFM) images to compare surface smoothness of the as-grown films quantitatively. In order to obtain reliable roughness data, the r.m.s. values of twenty different areas were averaged. Dielectric constant, dissipation factor, current density and polarization were measured to determine the electrical properties of the as-grown films. Thermal evaporated silver dots of an area of  $0.00385 \text{ cm}^2$  (diameter = 0.7 mm) were prepared on the as-grown films as the top electrodes. The substrates used were  $\langle 111 \rangle$  oriented platinum on Ti/SiO<sub>2</sub>/Si deposited by sputtering.

## 3. Results and discussion

### 3.1. Structural properties

The thickness of each film was estimated directly from cross-sectional SEM to be approximately 220 nm.

TABLE I Deposition condition of MOCVD grown- $\text{PbTiO}_3$  thin films

Parameters	Condition	Precursor	Parameter	Condition
Substrate temperature	$400^\circ\text{C}$	$\text{Pb}(\text{tmhd})_2$	Carrier gas flow rate	30 sccm*
	$480^\circ\text{C}$			
	$580^\circ\text{C}$			
	$580^\circ\text{C}-400^\circ\text{C}$			
Deposition pressure	$1.33-2.66 \times 10^2 \text{ Pa}$	Ti isoperoxide	Transport line temperature	250°C
Deposition time	1 h			
Deposition rate	$3.4 \text{ nm min}^{-1}$			
Carrier rate	Pure Ar gas			
Oxidizer	$\text{O}_2$		Carrier gas flow rate	5 sccm
			Bath temperature	$15^\circ$
			Transport line temperature	$250^\circ\text{C}$

\*SCCM: standard cubic cm per minute.

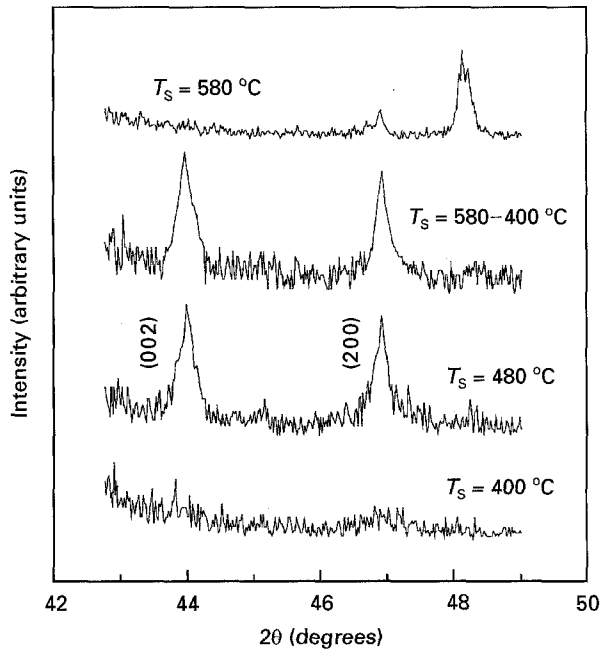


Figure 2 XRD patterns of  $\text{PbTiO}_3$  films deposited at 400 °C, 480 °C, 580 °C and by CCP.

Hence, the deposition rate was measured to be approximately  $3.65 \text{ nm min}^{-1}$ . The AES results showed that residual carbon was not detected and the ratio of the peak-to-peak intensities of all the films was similar to that of  $\text{PbTiO}_3$  film grown by MOCVD [7]. However, the WDS studies by using standard bulk  $\text{PbTiO}_3$  sample indicated Pb/Ti ratio of  $0.85 \sim 0.90$ , or Pb deficiency. Furthermore, near stoichiometry of oxygen was shown in the film deposited by the CCP, and slight oxygen deficiency was detected in the film at 480 °C. Fig. 2 shows the XRD patterns of 220 nm thick  $\text{PbTiO}_3$  films. The films deposited at 400 °C and 580 °C had poor crystallinity without any indication of tetragonal structure. Since 400 °C is not high enough for formation of crystalline film, the crystalline patterns of film deposited at 400 °C could not be shown. The poor crystallinity of the film deposited at 580 °C could be explained by instability of  $\text{PbTiO}_3$ -Pt interface at high deposition temperature. Although it can be easy to form crystalline nuclei at high substrate temperature, it can deteriorate the  $\text{PbTiO}_3$ -Pt interface by an interdiffusion, resulting in poor crystallinity at 580 °C. Polycrystalline perovskite structure with  $\langle 001 \rangle$  and  $\langle 100 \rangle$  direction normal to the substrate were shown in the films deposited at 480 °C and by the CCP. The crystallinity in the film by the CCP might have originated from nucleation formation characteristics and continuous cooling of deposition temperature. In general, a growth of crystalline film follows a formation of crystalline nuclei at an initial stage since the initial stage of nucleation can control film growth. Since 580 °C is high enough for the formation of crystalline nuclei, the crystalline nuclei could be formed preferentially at the initial stage. In spite of lowering the substrate temperature which can not form crystalline nuclei, the crystalline film could be grown by the crystalline nuclei formation. Therefore, the good crystallinity of the film by the CCP are due

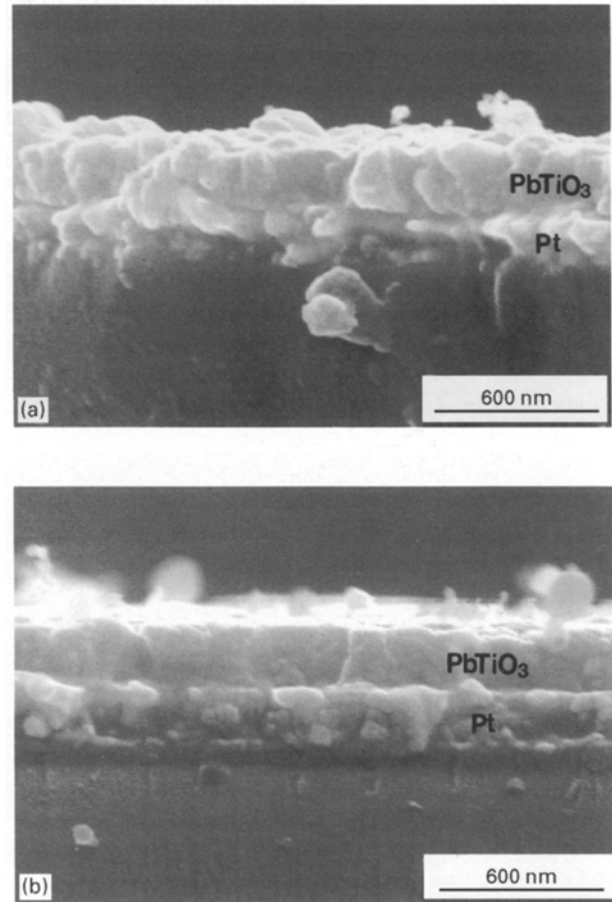


Figure 3 Interface structures of films deposited at 580 °C (a) and by CCP (b).

to the crystalline nuclei formation at the initial stage of the film formation, with growth temperature of 580 °C.

Fig. 3 shows interface structures of the films grown at 580 °C (a) and by CCP (b). There is severe interdiffusion at the interface of the  $\text{PbTiO}_3$ -Pt and the Pt-Si as shown in (Fig. 3a). It was reported that ferroelectric thin film deposition on Pt/Ti/SiO<sub>2</sub>/Si substrate had chemical instability of the bottom electrode at higher substrate temperatures. In the case of the film deposited by the CCP, there is not any interdiffusion of the bottom electrode toward the film as well as the Si substrate. The interdiffusion is ignored with decrease of the substrate temperature, resulting in sharp interface of  $\text{PbTiO}_3$ -Pt and Pt-substrate, and so good crystallinity, as mentioned in the XRD results.

The grain size of the film (Fig. 4d) by the CCP is larger than that of the film deposited at 400 °C (Fig. 4a) and 480 °C (Fig. 4b) as shown in the SEM photographs of film surface (Fig. 4). The grain size is very important because it can determine the final electrical properties of the film. The larger grain size is more favourable for real applications. The SEM images also show that the as-grown film by the CCP is more dense than the film deposited at 580 °C (Fig. 4c). These results suggest that the grain size and packing density of the film are strongly influenced by the initial stage of film formation. The nuclei size at higher substrate temperature usually tends to be larger, since nuclei formation at the initial stage of film formation is

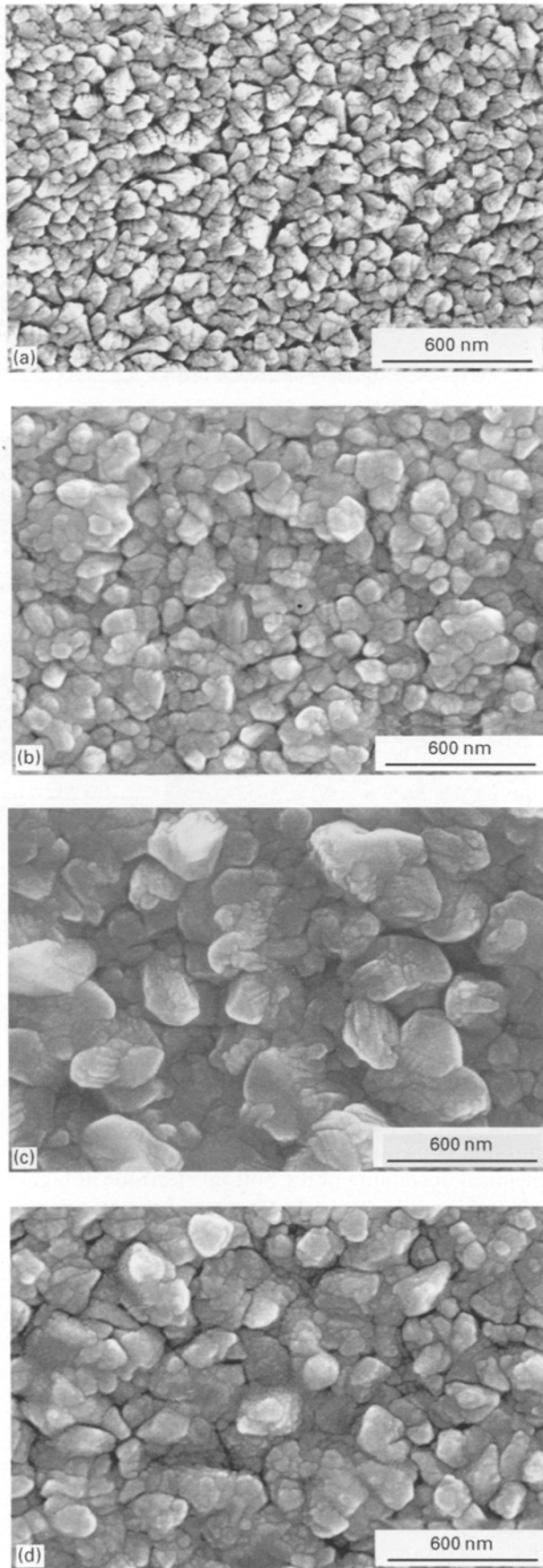


Figure 4 Surface structures of the films deposited at 400°C (a), 480°C (b), 580°C (c) and by CCP (d).

dependent upon surface migration of ad-atoms on substrate. Larger grains can occur in film growth with larger nuclei, since grains grow till they impinge on each of them. Therefore, the larger grain size of the

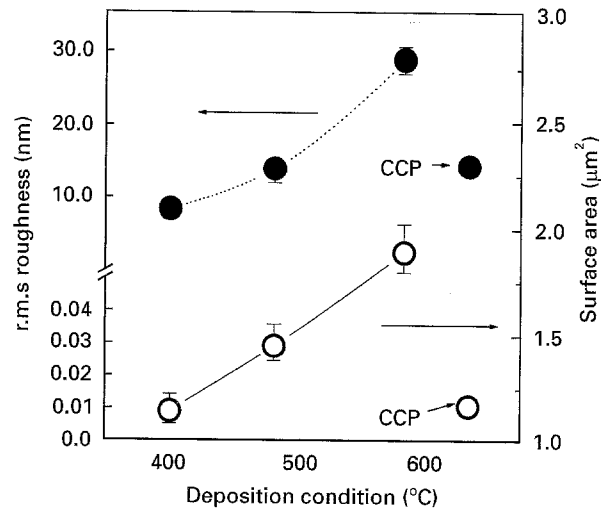


Figure 5 Root mean square surface roughness comparison for the film surface.

film by the CCP was caused by high starting substrate temperature of 580°C. Although very large grains were shown in the film grown at 580°C, these grains had poor crystallinity. Furthermore, lower packing density (Fig. 4c) might have originated from the chemical reaction during the deposition at the interface, as mentioned in the cross-sectional SEM images.

In order to compare surface roughness of the films, average root mean square (r.m.s.) roughness was measured from two-dimensional AFM images. Twenty different areas of the sample surface were scanned to obtain reliable r.m.s. roughness data. Fig. 5 shows r.m.s. roughness and surface area for the surface of each of the films. The r.m.s. surface roughness for the films deposited at 400, 480, 580°C and by the CCP are 8.4, 13.5, 29.5 and 14.0 nm over a distance of 1  $\mu\text{m}$ , respectively. The r.m.s. roughness increased with increase of substrate temperature. Comparison of the SEM and AFM results indicated that the increase of the surface roughness with increase of deposition temperature is caused by the grain growth at higher substrate temperature. Since grains can grow, not only parallel to substrate surface, but also perpendicular to it, the surface roughness could be increased in the case of film growth with the large grains. An abrupt increase of roughness in the film deposited at 580°C might be closely related to the low packing density and/or inhomogeneity of grain size. Although the detailed origin of inhomogeneous grain size for the film deposited at 580°C is not clearly understood as shown in Fig. 4, the higher surface roughness than that of the other films is due to the inhomogeneity of grain size. Furthermore, interface reaction of the  $\text{PbTiO}_3$ -Pt (shown in Fig. 3a) might give rise to the rough surface. In spite of the larger grain, the roughness of film deposited by the CCP was nearly the same as that of the film at 480°C. Since reduced surface area can reduce the surface energy of the film; a smooth film surface is achieved in the case of film growth with small surface area [20]. The AFM results also showed smaller surface area (1.16  $\mu\text{m}^2$  in scanning area of 1  $\mu\text{m}^2$ ) of the film deposited by the CCP than that

( $1.34 \mu\text{m}^2$  in scanning area of  $1 \mu\text{m}^2$ ) of film at  $480^\circ\text{C}$ . Therefore, the lower roughness of film by the CCP is due to the smaller surface area or higher packing density. However, it is not easy to conclusively understand that the main reason for the flat surface is caused by the small surface area. More systematic studies are needed to understand this phenomenon.

### 3.2. Electrical properties

Dielectric constant ( $\epsilon$ ) and dissipation factor ( $\tan \delta$ ) in frequency range of 0.3–1000 kHz were measured in order to investigate dielectric properties of the films. Since the applied electrical field can make a domain wall contribution at the polarization state for the dielectric properties, the lower electrical field ( $E$ ) than the coercive field of this material [21, 22] was applied to the films to prevent formation of the polarization state by the alternating current field. Fig. 6 shows the plots of  $\epsilon$  and  $\tan \delta$  as a function of frequency, which shows typical frequency dependence characteristic of a ferroelectric film having a metal–insulator–metal (MIM) structure. Namely, the dielectric constant of all the films decreased with increase of the frequency. In the frequency range of 0.3–1000 kHz, the dielectric constant of the films deposited at 400, 480, 580 °C and by the CCP were 60, 150–155, 90–145 and 180–240, respectively. The film deposited by CCP had the largest  $\epsilon$  than the other films in all frequency ranges, which may be associated with the crystallinity, large grain size and sharp interface, as shown in the XRD and the SEM results. The larger dielectric constant of the film deposited by CCP than the film at 480 °C is mainly due to grain size, and than the film deposited at 580 °C is owing to sharp interface as well as crystallinity. The increase of  $\tan \delta$  at frequencies above 100 kHz is caused by a contact resistance between the probe and the electrode [10, 23–25]. Not only the largest  $\epsilon$  but also the lowest  $\tan \delta$  were obtained for the film by the CCP. Although the film at 580 °C had a severe interface reaction and so interface broadening, the highest dissipation factor was observed in the film at 400 °C. The high dissipation factor in the film at 400 °C is generally observed in amorphous ferroelectric film. However, the reason for such phenomenon in dissipation factor between film at 400 °C and 580 °C is not yet clear. It was reported that more oxidized  $\text{BaTiO}_3$  film by multi-ion beam reactive sputtering had a lower dissipation factor [26]. As shown in the WDS results, the film deposited by CCP and at 480 °C had near oxygen stoichiometry and oxygen deficiency, respectively. Therefore, the lower dissipation factor of the film deposited by the CCP than the film at 480 °C might have been attributed to a more oxidized state or to lesser amounts of oxygen vacancies. In order to study insulating properties, room temperature current–voltage ( $I$ – $V$ ) measurements were also conducted on the films as a function of the electrical field. Current density ( $J$ )–electrical field characteristics of the films are shown in Fig. 7. All the films exhibit non-linear  $J$ – $V$  properties. Except for the film at 400 °C, the  $J$  of the films were linear at the low  $E$ , that is, the films exhibit ohmic natures. This

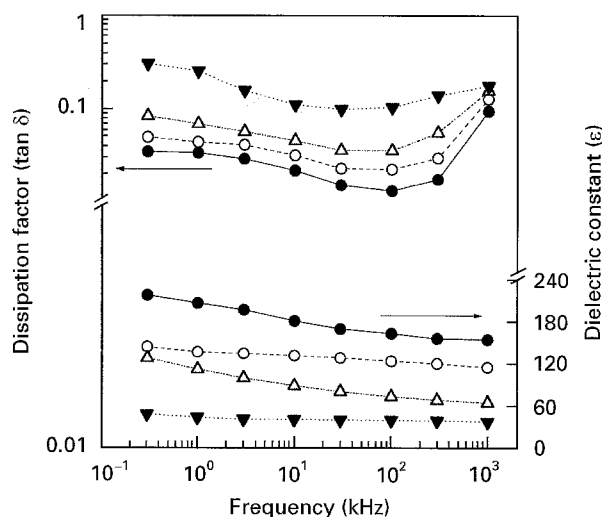


Figure 6 Dielectric constant ( $\epsilon$ ) and dissipation factor ( $\tan \delta$ ) as a function frequency.  $T_s$  = ( $\blacktriangledown$ )  $400^\circ\text{C}$ , ( $\circ$ )  $480^\circ\text{C}$ , ( $\bullet$ ) CCP, ( $\triangle$ )  $580^\circ\text{C}$ .

behaviour is consistent with a normal ferroelectric insulator. The  $J$  of the film by the CCP was lower than that of the film at  $580^\circ\text{C}$ . Higher values for the film at  $580^\circ\text{C}$  seems to be caused by formation of a mobile carrier arising from interfacial deterioration at high deposition temperature. Generally, leakage behaviours are closely related to (1) structural properties of the film such as crystallinity and density (intrinsic), and (2) extrinsic properties such as electrodes. Since the same electrode was used in this experiment, the lower  $J$  of the film by the CCP than that of the film at  $480^\circ\text{C}$  could be ascribed to an intrinsic property such as improved oxidized state leading to near oxygen stoichiometry. There are nonlinear  $J$ – $E$  relationships at the high electrical field. Around  $10^5 \text{ V cm}^{-1}$ , the  $J$  for the film by the CCP increases dramatically and becomes larger than that of the film at  $480^\circ\text{C}$ . This phenomenon was shown in  $\text{Bi}_4\text{Ti}_3\text{O}_{12}$  film annealed in  $\text{O}_2$  and  $\text{N}_2$  [27]. Such leakage behaviour could be understood by charge carrier traps. If a film has many carrier traps, the localized carriers at the traps begin to come out at high electrical field, resulting in abrupt increase of  $J$ . In general, the traps correspond to pores. Since the film by the CCP had higher packing density than the film at  $480^\circ\text{C}$  as shown in the AFM results, the reason for the higher  $J$  of the film by the CCP than that of the film at  $480^\circ\text{C}$  above the electrical field of  $10^5 \text{ V cm}^{-1}$  is not clearly understood. The difference of the  $J$ – $V$  plot in the film by the CCP and at  $480^\circ\text{C}$  might have originated from microstructural differences. A better understanding of the  $J$ – $E$  property can lead to explanation of the film structure. The leakage in ferroelectric can be described by two theories [28], (a) space charge limited conduction (SCLC) and (b) grain boundary limited conduction (GBLC). The  $J$ – $E$  plot of the film at  $580^\circ\text{C}$  was similar with that of the SCLC, and the films by the CCP and at  $400^\circ\text{C}$  exhibited the GBLC. However, the  $J$ – $E$  relationship of the film at  $480^\circ\text{C}$  could not be described by the above theory in the electrical field. More detailed works on the characteristics of the  $J$ – $E$  behaviours are underway.

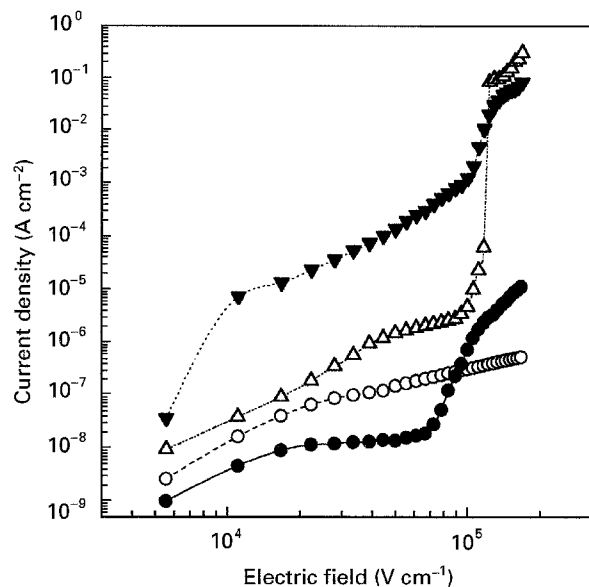


Figure 7 Current density ( $J$ )–electrical field ( $E$ ) characteristics of the films. ( $\nabla$ )  $T_s = 400^\circ\text{C}$ , ( $\circ$ )  $480^\circ\text{C}$ , ( $\bullet$ ) CCP, ( $\Delta$ )  $580^\circ\text{C}$ .

Ferroelectricity of the films was measured in terms of the polarization ( $P$ )–electrical field at frequency of 1 kHz with a computerized Sawyer–Tower circuit. Fig. 8 shows the typical  $P$ – $E$  hysteresis loops of the films. Perfect saturation was not shown in the loops of all films. This shape of the loops seems to be caused by non-stoichiometry of the films as shown in the AES and the WDS results. The ferroelectric loop was not shown in the film at  $400^\circ\text{C}$ , indicating that there was no formation of perovskite crystal phase as confirmed in the XRD results. Although the ferroelectricity was shown in the film at  $480^\circ\text{C}$ , the loop was slimmer than that of the film by the CCP. If the film has more oxygen vacancies, the hysteresis loop could become slimmer [29]. In other words, domain wall pinning is increased by increase in oxygen vacancy. As shown in the WDS results, the films at  $480^\circ\text{C}$  and by the CCP had oxygen deficiency and near oxygen stoichiometry, respectively. Therefore, the difference of the loop between the film at  $480^\circ\text{C}$  and by the CCP might be due to the oxygen vacancy. The slim loop of the film at  $580^\circ\text{C}$  might have resulted from the interfacial deterioration and reduction of the crystallinity as shown in the SEM and XRD results. Although this value is lower than that of bulk ( $P_r = 23 \mu\text{C cm}^{-2}$ ) [21, 22], in case of the film by the CCP, the measured remanant polarization was  $14 \mu\text{C cm}^{-2}$  which is higher than that of the film at  $480^\circ\text{C}$ . The higher  $P_r$  in the film by the CCP than the film at  $480^\circ\text{C}$  is related to the larger grain size of the film by the CCP than the film at

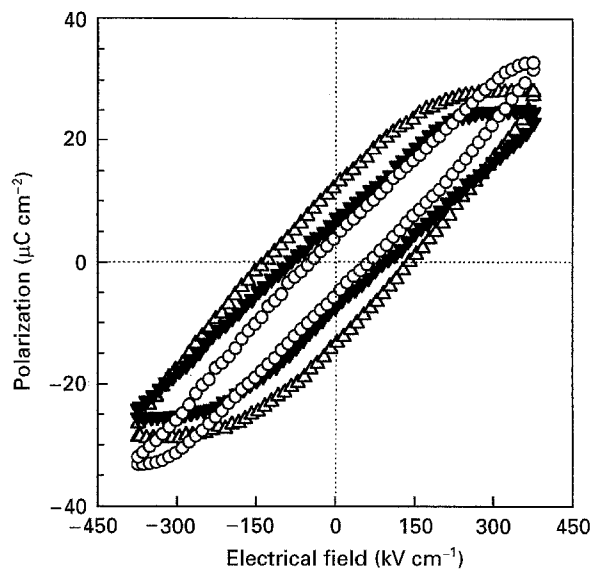


Figure 8 Typical polarization ( $P$ )–electrical field ( $E$ ) loops of the films. ( $\Delta$ )  $T_s = \text{CCP}$ , ( $\nabla$ )  $480^\circ\text{C}$ , ( $\circ$ )  $580^\circ\text{C}$ .

$480^\circ\text{C}$  [30, 31]. Conclusively, such better  $P$ – $E$  characteristics of the film by the CCP than the other film may also be attributed to improved packing density, larger grain and surface roughness as well as crystallinity as suggested in the dielectric properties. Comparison of dielectric and ferroelectric properties of  $\text{PbTiO}_3$  films deposited at various temperature and by the CCP are summarized in Table II.

#### 4. Conclusions

In order to investigate the possibility of the continuous cooling process as a new deposition method for thin film for many applications,  $\text{PbTiO}_3$  thin films were grown on a  $\text{Pt/Ti/SiO}_2/\text{Si}$  substrates at various growth temperatures by *in situ* metalorganic chemical vapour deposition. Even though it is not easy to conclusively explain the reason why CCP improves the crystallinity, the surface smoothness and the interface structure, it is speculated that crystalline nuclei were formed at the CCP starting temperature of  $580^\circ\text{C}$ , that is, initial stage of the film growth. The formations of nuclei at the initial stage can determine film growth characteristics and so the final properties of the films. The XRD, AFM and SEM observations prove the importance of the CCP for growth of high quality  $\text{PbTiO}_3$  film with good crystallinity, smooth surface and sharp interface. In the case of the film by the CCP, it is possible to improve not only the structural properties but also electrical properties.

TABLE II Comparison of dielectric and ferroelectric properties of  $\text{PbTiO}_3$  film deposited at various temperatures and by CCP

Condition	$\epsilon$	$\tan \delta$	$J$ ( $\text{A/cm}^2$ ) $\log E = 4.5$	$P_s$ ( $\mu\text{C/cm}^2$ ) 1 kHz	$P_r$ 1 kHz	$E_c$ ( $\text{kV/cm}$ ) 1 kHz
Range	(0.3–1000 kHz)	1 kHz				
$400^\circ\text{C}$	60	0.25	$3 \times 10^{-5}$			
$480^\circ\text{C}$	150–155	0.042	$9 \times 10^{-7}$	23	8	120
$580^\circ\text{C}$	90–145	0.06	$9 \times 10^{-5}$	30	4	100
CCP	180–240	0.023	$10^{-8}$	28–29	14	150

## References

1. M. D. CARPER and P. P. PHULE, *Appl. Phys. Lett.* **63** (1993) 163.
2. A. GRILL, W. KANE, J. VIGGIANO, M. BRADY and R. LAIBOWITZ, *J. Mater. Res.* **7** (1992) 3260.
3. G. R. BAI, H. L. M. CHANG, H. K. KIM, C. M. FOSTER and D. J. LAM, *Appl. Phys. Lett.* **61** (1992) 408.
4. G. H. HARTTLING, *J. Vac. Sci. Technol.* **49** (1989) 414.
5. M. de KEIJSER, G. J. M. DORMANS, J. F. M. CILLESSEN, D. M. de LEEUW and H. W. ZANDBERGEN, *Appl. Phys. Lett.* **58** (1991) 2636.
6. P. K. LRSEN, R. CUPPENS and G. A. C. M. SPRIERINGS, *Ferroelectrics* **128** (1992) 265.
7. J. F. SCOTT and C. A. PAZ DE ARAUJO, *Science* **246** (1989) 1400.
8. T. W. KIM, D. U. LEE, Y. S. YOON, S. H. WANG, S. S. YOM, S. J. LEE and C. O. KIM, *Solid State Commun* **96** (1995) 95.
9. K. IJIMA, Y. TOMITA, R. TAKAYAMA and I. UEDA, *J. Appl. Phys.* **60** (1986) 361.
10. K. SREENIVAS, A. MANSINGH and M. SAYER, *ibid.* **62** (1987) 4475.
11. Y. S. YOON, W. N. KANG, S. S. YOM, T. W. KIM, M. JUNG, H. J. KIM, T. H. PARK and H. K. NA, *Appl. Phys. Lett.* **63** (1993) 1104.
12. Y. S. YOON, D. H. LEE, T. S. KIM, M. H. OH and S. S. YOM, *J. Vac. Sci. Technol.* **12** (1994) 751.
13. Y. S. YOON, W. N. KANG, H. S. SHIN, S. S. YOM, T. W. KIM, J. Y. LEE, D. J. CHOI and S. S. BAEK, *J. Appl. Phys.* **73** (1993) 1547.
14. S.-G. YOON and H.-G. KIM, *J. Electrochem. Soc. Solid State Sci. Technol* **135** (1988) 3137.
15. H. NAKAZAWA, H. YAMANE and T. HIRAI, *Jpn. J. Appl. Phys.* **30** (1991) 2200.
16. B. S. KWAK, K. ZHANG, E. P. BOYD and A. ERBI, *J. Appl. Phys.* **69** (1991) 767.
17. L. A. WILLS, W. A. FEIL, B. W. WESSELS, L. W. TONGE and T. J. MARKS, *J. Cryst. Growth* **107** (1991) 712.
18. A. GRILL, D. BEACH, C. SMART and W. KANE, *Mater. Res. Soc. Proc.* **310** (1993) 189.
19. H. N. AL-SHAREEF, O. AUCIELLO and A. I. KINGON, *J. Appl. Phys.* **77** (1995) 2146.
20. L. I. MAISSEL and R. GLANG, "Handbook of thin film technology" (McGraw-Hill, New York, 1970).
21. T. OGAWA, S. SHINDOU, A. SENDA and T. KASANAMI, *Mater. Res. Soc. Proc.* **243** (1992) 93.
22. P. C. JOSHI and S. B. KRUPANIDHI, *J. Appl. Phys.* **72** (1992) 5827.
23. Y. S. YOON, Y. K. YOON and S. S. YOM, *Jpn. ibid.* **33** (1994) 6663.
24. M. H. FRANCOMBE, *Thin Solid Films* **13** (1972) 413.
25. K. OKAZAKI and K. NAGATA, *J. Amer. Ceram. Soc.* **56** (1973) 82.
26. C.-J. PENG, H. HU and S. B. KRUPANIDHI, *Appl. Phys. Lett.* **63** (1993) 734.
27. H.-J. CHO and T. W. NOH, *ibid.* **65** (1994) 1525.
28. H. HU and S. B. KRUPANIDHI, *J. Mater. Res.* **9** (1994) 1484.
29. W. L. WARREN, D. DIMOS and B. A. TUTTLE, *J. Amer. Ceram. Soc.* **77** (1992) 864.
30. C. V. R. VASANT KUMAR, R. PASCUAL and M. SAYER, *J. Appl. Phys.* **71** (1992) 864.
31. M. KLEE, R. EUSEMANN, R. WASER, W. BRAND and H. VAN HAL, *J. Appl. Phys.* **72** (1992) 1566.

Received 23 February  
and accepted 13 June 1996